DEVELOPMENT OF GOLD NANOPARTICLES DECORATED 3D GRAPHENE FOAM AS AN ULTRA-SENSITIVE AND LABEL-FREE NEUTROPHIL GELATINASE ASSOCIATED LIPOCALIN ELECTROCHEMICAL SENSOR FOR ACUTE KIDNEY INJURY DETECTION

by

Pobporn Danvirutai

A Dissertation Submitted in Partial Fulfillment of the Requirements for the Degree of Doctor of Engineering in Microelectronics and Embedded Systems

Examination Committee:	Dr. Mongkol Ekpanyapong (Chairperson) Dr. Adisorn Tuantranont Dr. Huynh Trung Luong
External Examiner:	Prof. Carlos Manuel José Alves Serôdio Engineering Department Universidade de Tras-os-Montes, Portugal
Nationality:	Thai
Previous Degree:	Master of Engineering in Computer Science Asian Institute of Technology Thailand
Scholarship Donor:	AIT-Fellowship

Asian Institute of Technology
School of Engineering and Technology
Thailand
December 2021

AUTHOR'S DECLARATION

I, Mr. Pobporn Danvirutai, declare that the research work carried out for this dissertation was in accordance with the regulations of the Asian Institute of Technology. The work presented in it are my own and has been generated by me as the result of my own original research, and if external sources were used, such sources have been cited. It is original and has not been submitted to any other institution to obtain another degree or qualification. This is a true copy of the dissertation, including final revisions.

Date: 14 September 2021

Name: Pobporn Danvirutai

Signature: 

ACKNOWLEDGMENTS

This work is dedicated to the memories of my father, Assist. Prof. Paiboon Danvirutai who always gave warm supports and encouragement. I would also much thankful to Assoc. Prof. Chanaiporn Danvirutai for infinite supports. This research work is also dedicated to the memories of Assoc. Prof. Erik Bohez and Dr. Pornpimol Srithongkham, my ex-coadvisors who guided the work in the past.

I deeply indebted to Dr. Chavis Srichan who has kindfully helped me by initiating the topic, gave suggestions, guided, provided knowledge and motivated my studies since bachelor's degree until now. He contributed a lot to this research. Without him, this work would not be able to accomplish.

I would express a heartfelt thanks to my advisor, Assoc. Prof. Mongkol Ekpanyapong who always give me supports, guidance and helps in much many ways. Collaboration at NSTDA were very much sincerely acknowledged, especially the kindfulness of Dr. Adisorn Tuantranont and Dr. Anurat Wisitsoraat. I would thank Assoc. Prof. Luong for being my co-advisor after the passing of Assoc. Prof. Bohez. I am much thankful for helps from Mr. Ditsayut Phokaratkul, Ms. Patiya Pasakon and Dr. Saifon Kullayakool for instrumental and technical supports.

Collaboration at Khon Kaen University were much acknowledged, especially, Assoc. Prof. Pittayakorn Noisong, Dr. Nawapak Eua-Anant, and Mr. Mahattanah Kowsuvun. I would also gratefully thank to supports from CKDNET-KKU especially Assoc. Prof. Sirirat Anutrakulchai, for substance preparations, topic motivations and supports.

The work was financially supported by AIT Fellowship Scheme and Chronic-Kidney-Disease care in North-East Thailand (CKDNET), Khon Kaen University.

ABSTRACT

This dissertation reports an investigation of an ultra-sensitive and highly-specific electrochemical immunosensor development based on three-dimensional graphene/nickel foam (GF) decorated with gold nanoparticles (AuNPs) for the detection of Neutrophil Gelatinase Associated Lipocalin (NGAL), a biomarker of Acute Kidney Injury (AKI). A low NGAL limit of detection (LOD) of 42 pg/ml and a linear range (LR) of 0.05-210 ng/ml were achieved. Though several electrode platforms have been proposed, either LOD or LR are limited for each method. Our platform can achieve low LOD while keeping broad LR of sensing. Specificity was tested for NGAL detection against uric acid and creatinine interference. The attained performances might be ascribed to large specific surface area of GF and AuNPs, improved electron transfer from analyte via graphene-nickel-gold electric dipole enhancement. The results demonstrated the proposed platform was potential for ultra-sensitive, highly specific, non-invasive and real-time electrochemical detection of NGAL. At the first stage, concentrated NGAL solution was purchased to test sensitivity and specificity and was reported in Danvirutai *et al* (2020). Finally, this platform has been tested with 5 genuine urine samples of NGAL sensing which form a trend of the sensor at the trace amount of urine NGAL. This platform presents a promising approach for non-invasive and near real-time renal state monitoring.

Keywords:

Neutrophil Gelatinase-Associated Lipocalin, NGAL, electrochemical sensing, amperometric detection, cyclic voltammetry, 3D graphene foam, gold nanoparticles, noble-metallic dipole enhancement

CONTENTS

LIST OF TABLES

LIST OF FIGURES

LIST OF ABBREVIATIONS

AKI	=	Acute Kidney Injury
CKD	=	Chronic Kidney Disease
CV	=	Cyclic Voltammetry
GF	=	Graphene Foam
AuNPs	=	Gold Nanoparticles
LCN2	=	Lipocalin-2
NGAL	=	Neutrophil Gelatinase-Associated Lipocalin
Anti-	=	Antibody
FE-	=	Field-Emission Scanning Electron Microscope
SEM	=	Scanning Electron Microscope
XRD	=	X-Ray Diffraction
CVD	=	Chemical Vapour Deposition
i	=	Faradaic Current

CHAPTER 1
INTRODUCTION

1.1 Background

A very large number of people in the globe suffered from Chronic Kidney Disease (CKD), e.g., 15% of adults in the United States (according to CDC.gov 2021) and 17.6% in Thailand, that counts 8 millions people of the country. CKD has a strong correlation with Acute Kidney injury (AKI). Multiple occurrences of AKI promote CKD, and CKD people are more susceptible to AKI occurrence than normal people. Therefore, prevention and good care of AKI can reduce the risk of getting CKD.

In recent years, Neutrophil Genatenase-Associated Lipocalin (NGAL) gained much attention for its much faster response to Acute Kidney Injury (AKI) compared to traditional biomarkers such as creatinine. NGAL level increases in response to AKI within two hours whilst creatinine requires at least 6-8 hours to response. Therefore, the more accurate and real-time determination of NGAL level greatly help nephrology doctors to response faster and more affectively.

There are several candidates for NGAL electrochemical sensing mainly based on antibody with different modifications on electrode materials. In this work, we investigate the use of novel 3D graphene/nickel foam (GF) decorated with gold nanoparticles (AuNPs) as well as self-assembled Monolayers (SAM) with NGAL antibody (Anti-LCN2). Large surface area of 3D GF supports broad sensor reactive range and the dipole enhancement between graphene-nickel-gold greatly enhance sensitivity.

The NGAL level in urine of greater than or equal to 100 ng/ml can identify AKI with a very high confidence level (Cruz *et al*., 2010; Nickolas *et al.*, 2012) since the NGAL level in urine for normal people is in the range of 9-49.41 ng/ml or 5.7-17.7 ng/ml depending on age and other physical conditions (Makris & Spanou, 2015; Mishra *et al.*, 2005). The normal or abnormal NGAL level will eventually be decided by Nephrologists. Ultra-sensitive, highly-specific and real-time sensor is thus required.

Graphene, a single layer of carbon atoms bound in a hexagonal honeycomb lattice, is a valuable two-dimensional (2D) nanomaterial for a wide range of technological applications owing to its extraordinary physical and chemical properties (Novoselov *et al.*, 2004). In particular, possessing large surface area per mass and gigantic electron mobility associated with its massless Dirac electrons cause graphene highly sensitive for electrochemical detection and other electron-transfer-based sensing. Graphene-based electrochemical sensors have been demonstrated to exhibit ultrahigh detection sensitivity for several biochemical analytes (Ma *et al.*, 2014; Wu *et al.*, 2013). However, 2D graphene sheets commonly suffer from poor stability due to aggregation and restacking. An effective solution to the problem is to construct well-defined 3D graphene networks based on 2D graphene building blocks, providing stable intrinsic graphene properties (Chen *et al.*, 2011). 3D porous graphene structures can be fabricated by various solution syntheses and template growth based on chemical vapor deposition (CVD). Solution methods typically produce low-quality structures with discontinuous graphene interconnection and structural defects, limiting the use in some applications. In contrast, template-growth CVD processes can synthesize 3D graphene foam (GF) structures with seamlessly interconnected high-quality graphene layers exhibiting large effective surface areas (Zhang , Zhou & Zhao, 2010; Stoller *et al.*, 2008). In addition, 3D structure of graphene folded in Ni foam templates can be used as freestanding electrochemical electrodes with enhanced sensitivity due to large amount of graphene/nickel dipoles (Zhang *et al.*, 2018) and can support functional with gold nanoparticles (AuNPs) as well as for SAM and antibody conjugated binding. The more surface area for reaction, the more sensitivity achievable. Due to dipole enhancement, the reactive current gain is greatly increased. Biochemically decorated antibody on AuNPs ensure the specificity of the sensor.

GF were modified by several noble metallic nanostructures to work as highly sensitive biosensors, for example, AuNPs/ZnO nanocone array / GF for highly sensitive dopamine sensor (Yue *et al.*, 2020). GF electrode embedded with In_2O_3 nanosheet arrays was reported for dopamine determination under interference by uric acid (Guo *et al.*, 2020a). In addition, In_2S_3 has been used instead of In_2O_3 as nanosheet arrays on GF for epinephrine detection (Guo *et al.*, 2020b). In the previous study, nanosheet arrays / GF, the platforms achieved 0.1 uM and 0.12 uM LOD consecutively. Mycobacterium tuberculosis detection by sensing its DNA sequence using gold

nanorods on GF was reported with satisfactory linear range of 10 fM to 0.1 µM (Perumal *et al.,* 2018). Graphene/Nickel foam decorated by Iron nanoflorets was applied as an ultra-sensitive sensor for dangerous toxins, for example, sensing Deoxynivalenol (DON). The GF/Iron nanoflorets electrode attained LOD 2.11 pg/ml (Ong, *et al.*, 2020). GF/functionalized with different nanostructures for biosensing have been reviewed, then we focus on NGAL electrochemical sensing in literature.

Kannan, Tiong, and Kim (2012) proposed using label-free immunosensor utilizing AuNPs-generation-1polyamidoamine on top of gold electrode and achieved a detection limit of 1 ng/ml with wide linearity range of 50–250 ng/ml NGAL. Chen and Lu (2018) reported that using boron-carbon nitride electrode with Anti-LCN2 could achieve extremely-low detection limit of 0.37 pg/ml but suffer from limited linearity range of 0.001-10 ng/ml and thus require times for specimen dilution processes before sensing can be carried out. Neves et al (2020) achieved a very low LOD of 97 pg/ml using enzyme-based sandwich techniques, with limited linear range of 0.15-2 ng/ml though (Neves *et al.*, 2020).

In previous reports, either LOD or linear operation range cannot be optimized at the same time. We thus proposed novel 3D Graphene/Nickel foam functionalized with AuNPs and SAM-Antibody bounded to overcome the previous sensor limitations. The gigantic surface area of 3D graphene foam and AuNPs should be an effective mean to achieve ultra-sensitive and broad working range electrochemical NGAL immunosensors since electrochemical sensitivity will be enhanced due to induced electric dipoles at the interfaces between AuNPs and 3D graphene/Ni foam (Zhang, *et al.*, 2018; Kannan, Tiong & Kim, 2012). However, there is still no report of electrochemical NGAL sensors based on AuNPs/3DGF structures. In this work, electrodes based on GF/AuNPs were fabricated by CVD and electrodeposition processes as well as biochemically decorated with Lipocalin-2 antibody and investigated its performance as NGAL electrochemical sensor.

1.2 Statement of the Problem

1.2.1 A classic biomarker for AKI was creatinine, which response within 6-8h since the onset of AKI. Whilst, Neutrophil-gelatinase associated lipocalin (NGAL) response within 2 hours and can be measured from both urine and blood.

1.2.2 In order to achieve a quick response treatment for AKI, a quick-response biomarker must be picked. This work aim for developing NGAL sensors based on electrochemical using novel nanomaterials.

1.2.3 NGAL sensing platforms available in the literature could achieved either good sensitivity or broad linearity range, but not both. We aim to achieve both sigh sensitivity, selectivity and broad linearity range.

1.2.4 3D Graphene/Nickel foam form a highly sensitive electrode due to graphene-nickel dipole enhancement, gold nanoparticles and LCN2 antibody was added for specificity reason and form another layer of dipole between Au and graphene. Sensitivity, specificity and repeatability was reported.

1.3 Objectives

1.3.1 Develop a platform for NGAL determination based on novel nanomaterials electrode in electrochemical sensing

1.3.2 Test and compare the performances (sensitivity, selectivity, and working range) against other platforms.

1.4 Scopes and Limitations

1.4.1 Neutrophil-gelatinase associated lipocalin (NGAL) response within 2 hours, after AKI occurred, and can be measured from both urine and blood. Meanwhile, ordinary creatinine requires 6-8h to response. This work focus on development of sensing platform for NGAL determination.

1.4.2 Fast medical response to AKI occurrence requires a quick-response biomarker. Novel GF/AuNPs/Anti-LCN2 was proposed as a highly sensitive and selective electrode for NGAL determination as the AKI monitoring purpose.

1.4.3 In literatures, NGAL sensing platforms could achieved either high sensitivity or wide linearity range, but not both at the same time. Goal of this work is to fill the gap by achieving both sigh sensitivity, selectivity and broad linearity range.

1.4.4 3D Graphene-nickel dipole enhancement offers gigantic sensitivity.

However, to achieve high selectivity, AuNPs and LCN2 antibody was added. In addition, Au-G-Ni form triple-layer dipole enhancement, as the sensing performance reported in the next chapters.

1.5 Dissertation Outline

The first chapter explained motivations, introductions and statement of the problem. The second chapter presented conceptual background and literature review of related electrochemical sensing platforms. The third chapter explained synthesis and methodology. The fourth chapter provide primary results. The fifth chapter reports results in actual human urine NGAL determination. The last chapter provide the research conclusion.

CHAPTER 2
ELECTROCHEMICAL SENSING AND NOVEL ELECTRODES

This chapter reviews concepts and techniques of electrochemical detection in various platforms. Electrochemistry or voltammetry in general before we going deeper into electrochemical sensors. The reasons of using the proposed method in the dissertation will be explained along with this section.

2.1 Electrochemical Sensing

Electroanalytical methods can be divided into several categories: (i) Potentiometry, (ii) Coulometry, and (iii) Voltammetry. Our developing sensor platform falls into the third categories, voltammetry.

Figure 2.1

Basic Electrochemical Setup for Au(III) Electrodeposition onto GF

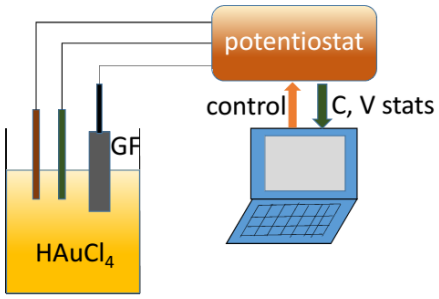

Most of electrochemical setup compose of three electrodes: (i) working electrode – where potential will be applied and reaction occurs, (ii) reference electrode – acting as a ground potential compared to working electrode potential and (iii) counter electrode – to complete electrical circuits.

In figure 2.1, GF was set as the working electrode and negative potential is applied in order to reduce gold ions (Au^{3+}) onto GF surface. For other purpose, electrochemical sensing also employed three-electrode system. Most of literature, the differences are the working electrode being used to sense analyte, it can be gold nanorods, carbon nanotubes, graphite, screen-printed carbon electrodes, antibody-decorated materials and so on.

Electron transfer results in reduction and oxidation reaction. The process causes changing in oxidation number of the elements in the materials. Oxidation reaction is the process of losing electrons. It can be written as

$$A \rightarrow A^{+} + e^{-}.$$

Reduction reaction is the process of gaining electron, i.e.

$$B + e^{-} \rightarrow B^{-}.$$

Redox = Reduction + Oxidation, for example, combining two reactions above gives

$$A + B \rightarrow A^{+} + B^{-},$$

during which the electron was transferred from chemical subject A to B. Since the reaction can be divided into reduction and oxidation, cyclic voltammogram shows two peaks of current occurred due to reduction and oxidation. Oxidation current (i_{pa}) and reduction current (i_{pc}) are shown in figure 2.2a. In electrochemical sensing, the peak of electron transfer current in a redox process determines the concentration of an analyte involved. Therefore, by fixing the applied potential at the oxidation potential, we can measure analyte's concentration by measuring the peak current (ampere). This work reports performance of using GF/AuNPs/AntiLCN2 as an active electrode to determine the concentration of NGAL.

A potentiometric sensor aims for determination of the concentration of an analyte gas or solution. Electrical potential of an electrode is measured when no current appears. The potential difference between working electrode and reference electrode is measured as the signal.

The working electrode's potential has to be proportional or one-direction function of the analyte concentration. Figure 2.2 shown three different potential setup in electrochemical sensing. Periodic rectangular potential is applied, sweeping through oxidation and reduction potentials of analyte in Fig. 2.2(a) – Cyclic Voltammetry (CV). Oxidation and reduction current in CV is proportional to concentration of analyte, in which oxidation and reduction was swept though and redox current found in cyclic voltammogram.

In figure 2.2(b), combined constant and linear sweep was applied in anodic stripping voltammetry – specific voltage will unbounded and oxidized a targeted particle. Whereas, in figure 2.2(c), potential was fixed and the current against time was plot

where dropping of analyte into the prepared solution was done at a certain time causing response current proportional to analyte concentrations.

Figure 2.2

Three Different Electrochemical Schemes

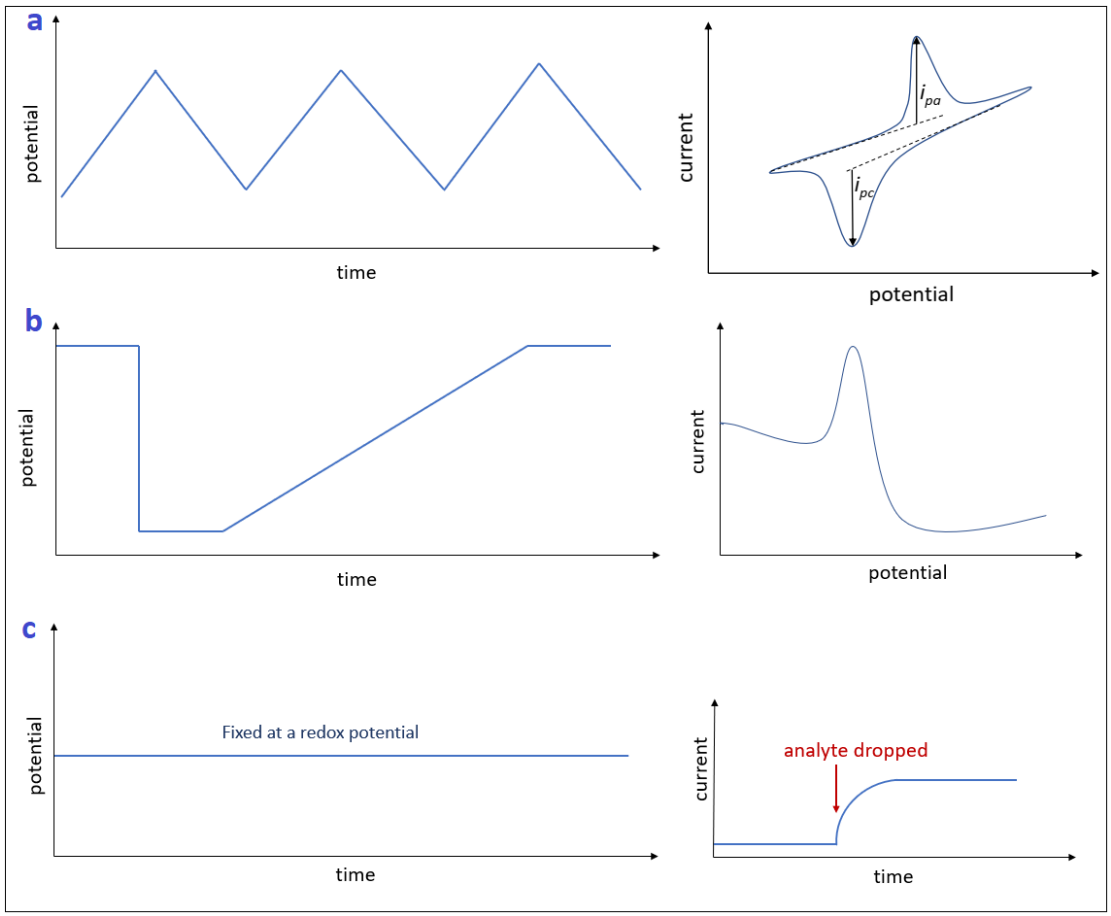

Note: (a) Cyclic Voltammetry (b) Anodic Stripping Voltammetry and (c) Chronoamperometry.

The field pioneered by Jaroslav Heyrovský on polarographic techniques which granted him 1959 Nobel Prize in Chemistry. Polarography is an electromechanical technique for measuring concentration of analyte by measuring current flows between two electrodes in the solution while applied potential is gradually increasing. Whilst, in polarography, the applied potential is only linearly increasing form; voltammetry, on the other hand, modifies applied potential in different ways: cyclic triangular wave (CV), hybrid constant and linear potential (Stripping Voltammetry) periodic rectangular wave form (Square-Wave Voltammetry: SWV), constant potential together

with linear potential drop (Anodic stripping voltammetry). Among many different proposed of applied potential, cyclic voltammetry is one of the most popular technique due to its continuous potential sweep that gather both reduction and oxidation current characteristics. In cyclic voltammetry, the faradaic current occurs is explained in section 2.1.1.

Common voltammetric techniques involve applying potential (E) into electrodes and measure the oxidation or reduction current flowing in the electrochemical cell system. In voltammetry, potential is varied in a range and the potential (E), current (I) and time (t) is plotted. In amperometry, a potential is fixed constant and current is plot against time to detect redox reaction occur in the cell at a specific potential. This amperometric technique is applied to sense analyte and thus called amperometric sensors. In amperometry, faradaic current is described by Cottrell equation, i.e.,

$$i = \frac{nFAC\sqrt{D}}{\sqrt{t\pi}}$$

where *F* is the Faraday constant (96485 Coulomb/mol), *C* is the initial concentration of a reactive agent, *D* is the diffusion coefficient, *n* is the number of electrons, *A* is the reactive area of the electrode and *t* is the time (s). Since graphene has extraordinary high surface area per mass and the term A incorporate linearly into current, extremely-high sensitivity can be achieved in graphene-based electrodes. In addition, given other parameters known, current is proportional to analyte concentration. Measuring the current thus also determine the concentration of analyte.

In coulometry the amount of matter transformed during an electrolysis is determined by measuring the amount of electricity (in coulombs) consumed or produced. It was used as a precision measurement for charge, and charge transfer, the method is named in honour of Charles-Augustin de Coulomb. There are two basic coulometric approaches. First, potentiostatic coulometry in which applied potential is fixed during the reaction. Second, amperometric coulometry keeps the current constant by coulometric titration using amperostat.

2.1.1 Cyclic Voltammetry

Cyclic Voltammetry (CV) is among several types of voltametric techniques where applied potentials are swept in several ways, square-wave signals, constant and linear

form (stripping voltammetry). In this work, we use cyclic voltammetry in order to find the potential yielding optimal redox current. After that, we fixed the applied potential and measure the concentration in chronoamperometry.

The peak current in cyclic voltammogram can be formulated according to Randles–Ševčík equation:

$$i_p = 0.4463\, nFAC\left(\frac{nFvD}{RT}\right)^{\frac{1}{2}}.$$

where n is the number of electrons transferred per one reaction (usually 1),

F is the Faraday constant (C mol^{-1})

A is the surface area of electrode (cm^2)

C is the concentration of analyte (mol/ml)

D is the diffusion coefficient in cm^2/s

R is the gas constant (J K−1 mol−1)

T is the temperature in Kelvin.

To be specific, at room temperature (25 °C), current becomes

$$i_p = 2.69 \times 10^5\, n^{\frac{3}{2}} AD^{\frac{1}{2}} Cv^{\frac{1}{2}}$$

Considering surface area (A) using graphene gives extraordinary increasing of sensitivity due to its gigantic surface area per mass (2600 m^2/g) (Sur, 2012). Once all parameters are fixed, current would be linearly proportional to analyte concentration. These are how the platform can determine analyte (NGAL) concentration.

2.1.2 Chronoamperometry

There are two types of chronoamperometry: controlled-potential and controlled-current. We apply controlled-potential chronoamperometry to determine the concentration of analyte. However, before conducting this, cyclic voltammetry need to be run in order to find the reduction and oxidation potential.

Once cyclic voltammetry was conducted, we would know reduction and oxidation potential of analyte. Picking a voltage that yield highest reduction current. Fixing the applied potential to the reduction point, and measuring reactive current vs time is called

chronoamperometry. This work we conducted chronoamperometry for NGAL by dropping into the solution and measure the current. To test specificity, other chemicals, i.e., uric acid and creatinine are dropped and measure interference. Once analyte solution is dropped into the prepared solution, faradaic processes occurs at the electrodes causing the amperometric current measured at an potentiostat instrument. Current response and time was form as a function I(t, c), where response patterns correspond to time and concentration of analyte dropped into solution standing on top of a magnetic stirrer. Amplitude of the steady current response formed linear relationship with each dropped concentrations. This functional relationship enables us to apply the platform as electrochemical determination of an analyte.

2.1.3 Mediated Amperimetric Biosensing

Ferri/ferrocyanide redox is written as

$$[Fe(CN)_6]^{4-} \leftrightarrow [Fe(CN)_6]^{3-} + e^-$$

Ferri/ferrocyanide redox system was applied in the research to act as an electron mediator towards and backwards from analyte and the electrode surface. Other charged molecule system can also act as a mediator but ferri/ferrocyanide was commonly used due to its symmetric shape in cyclic voltammogram.

2.1.4 Electrochemical Impedance Spectroscopy

In electrochemical impedance spectroscopy (EIS), alternating current resistance of electrochemical system is measured. Impedance spectroscopy is conducted by applying an alternating voltage, i.e., the potential at the working electrode is modulated sinusoidally and the current and its phase will be measured.

Charge-transfer impedance is inversely proportional to the redox current amplitude. The impedance can be measured in Electrochemical Impedance Spectroscopy (EIS). Charge transfer resistance (R_{ct}) is formulated by

$$R_{ct} = \frac{RT}{nFI_o}$$

where R is the gas constant, T is the temperature, n is the number of electrons involved, F is the Faraday constant, and I_0 is the exchange current density.

2.2 Electrochemical Deposition

Reduction process of noble metal ions onto an electrode can form a fruitful platform for nanoparticles decoration process. In our work, we applied negative potential into graphene foam electrode in order to reduce Au^{3+} into GF surface and formed distributed gold nanoparticles all around GF surface sites.

2.3 Novel Electrode Materials for Electrochemical Sensing

Carbon-based electrodes usually hold promising properties such as high conductivity, high surface area and the stability. Among the carbon materials, graphene or single-atom thick of graphite yields highest conductivity, and highest electron mobility (speed of electron is approaching speed of light, requiring relativistic quantum mechanics to explain). Carbon-nanotubes (CNT) or folded geometry of graphene into a tube shape is also used. However, in our work, CNT has no interlayer dipole enhancement like those in Au-GF-Ni layers in our work (Zhang et. al., 2018).

Combined carbon-based and nanoparticles electrodes. Several materials has been proposed for achieving high sensitivity in electrochemical, e.g., bare gold +AuNPs and enzymes, flat graphene and polyanilene sensing and these will be compared in chapter 4 in the performance for NGAL sensing.

NGAL (Lipocalin 2) Sensor

Lipocalin-2 (LCN2) is a biomarker for many inflammatory-based diseases, including acute kidney injury, cardiovascular stress, diabetes, and various cancers (Zhai *et al*, 2012). The more effective (rapid, sensitive, selective and non-invasive) determination of NGAL level implies more efficacy in AKI treatment before the case becomes severe. Traditional method for NGAL sensing is via ELISA where sensing is limited in short linear range 0.004-1 ng/ml. This method requires several dilution processes before the sample can be measured. In this work, we reported a platform for sensing at hundred times broader range with high sensitivity and selectivity.

CHAPTER 3

MATERIALS AND METHODS

3.1 Structural Characteristics of GF/AuNPs

The typical structural characteristics of GF/AuNPs are reported in Fig. 3.1(a-d). In fig. 3.1a demonstrates a thin and long strip of GF/AuNPs with a flexible gray sponge appearance. The optical micrograph (Fig. 3.1b) displays inter-connecting bridge networks with a bright gray color of graphene-coated partially etched nickel foam having open pores with diameters in the range of 50–300 μm. The related low-magnification FE-SEM micrograph (Fig. 3.1c) illustrates 20–40 μm wide smooth lamellae of the foam network exhibiting fine particulate surface textures. The corresponding magnified FE-SEM image (Fig. 3.1d) reveals a wrinkle surface morphology of GF decorated quite uniformly with a number of bright particles having varying diameters. The particle size distribution (Fig. 3.1e) determined using an imaging analysis based on a MATLAB code shows that more than 70% of all nanoparticles have diameters between 45 and 55 nm with the mean value of 50.1 nm and the standard deviation of 4.23 nm, indicating that the electrodeposition process can produce gold nanoparticles with well-controlled size on GF.

Figure 3.1

(a) Photograph, (b) Optical Micrograph, FE-SEM Images at (c) Low and (d) High Magnifications of GF/AuNPs, and (e) Size Distribution of AuNPs Deposited on GF.

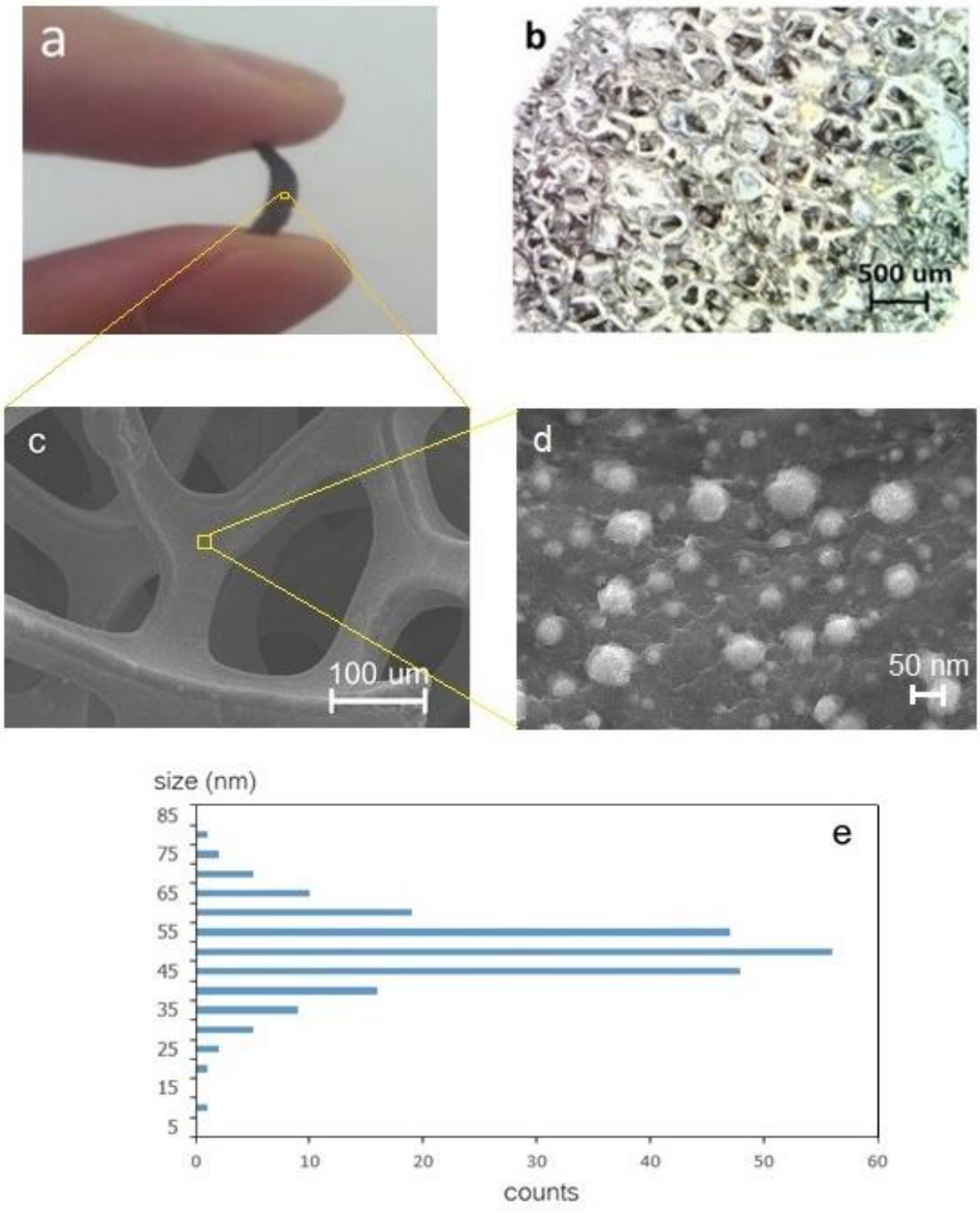

Figure 3.2

Characterization of GF/AuNPs using (a) Raman Spectrum and (b) XRD

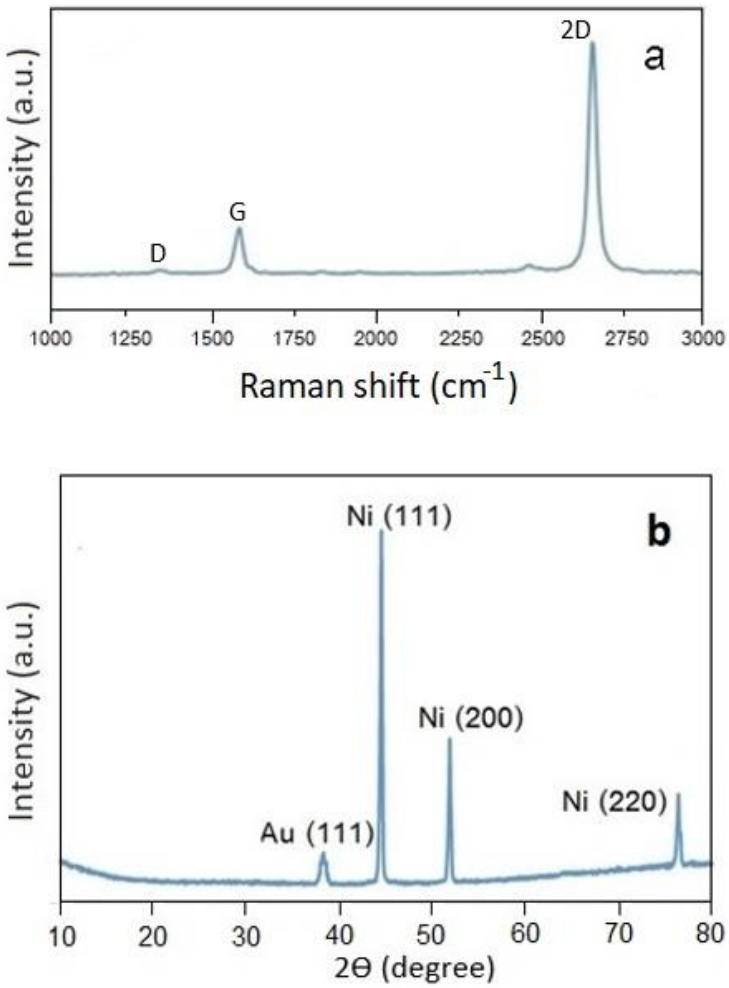

The chemical information of GF/AuNPs provided by Raman spectroscopy and X-Ray diffraction are presented in Fig. 3.2b. The Raman spectrum of AuNPs/GF (Fig. 3.2a) displays three graphene-related characteristic peaks including D, G and 2D at 1330, 1574 and 2648 cm^{-1}, respectively. Apparently, the 2D peak is more than three times as high as the G peak, signifying the presence of monolayer graphene. In addition, the D band magnitude is very low compared with G and 2D, indicating very low amount of edge defects and high quality of the CVD graphene. There is no Raman peak of other components of GF/AuNPs including Ni and Au because they are not Raman active. In contrast, the corresponding XRD pattern (Fig. 3.2b) demonstrates the peaks associated with Ni and Au phases while the peaks related to graphene are absent because the amount of graphene is very low. The Au (111) peak at 38.1° is relatively low in

magnitude compared with Ni in accordance with its low content. The result evidently confirms the presence of AuNPs on GF.

3.2 Material Synthesis and Characterization

3.2.1 Fabrication of 3D GF

Graphene/Nickel foams were fabricated using the CVD process similarly to (Srichan *et al.*, 2016). The CVD 3D GF fabrication utilized hydrogen (H_2) and acetylene (C_2H_2) as the reducing agent and the carbon precursor for GF synthesis on nickel (Ni) foam, respectively. Firstly, H_2 was passed through Ni foams placed at the center of a horizontal tube furnace in vacuum at a pressure of 1 Torr and a temperature of 700 °C for 30 minutes. Next, the C_2H_2/H_2 mixture (1/8) was introduced shortly at 0.2 Torr for 3 minutes followed by the resumption of hydrogen flow at 1 Torr and the rapid cooling step using a moving furnace technique achieving a cooling rate of more than 10 °C per minute. During the rapid cooling period, carbon atoms from C_2H_2 dissolved on Ni surfaces would segregate into graphene layers on the Ni scaffold (Figure 3.3). Finally, the graphene/nickel foams were immersed in a 3M HCl solution at 60°C for 30 min to partially etch the nickel foams and obtain GFs with some remaining Ni.

Figure 3.3

Chemical Vapour Deposition Setup for Fabrication of Graphene/Nickel Foam.

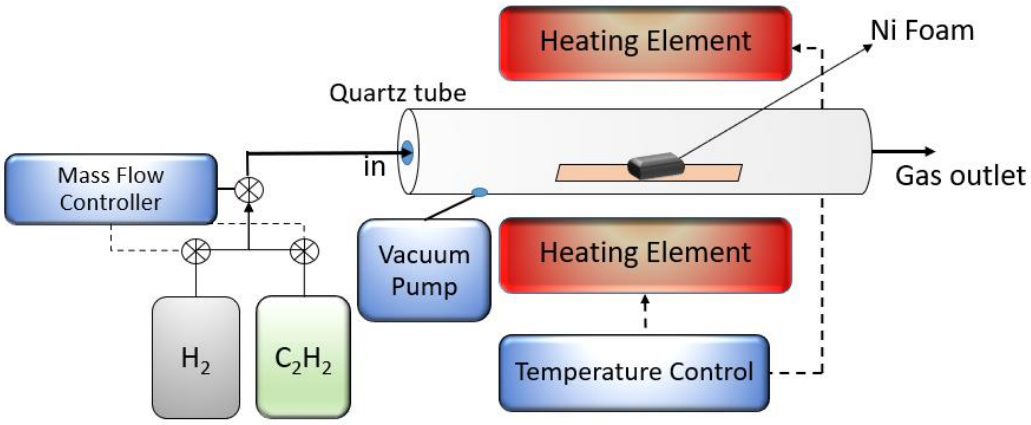

Note. Ni Foam was placed inside the quartz tube then being heated upto 700 C at 1 Torr pressure, C_2H_2 is flow through the tube as precursor for carbon atom deposition. Very

fast cooling cause carbon atoms formed as 3D graphene layer on the surface of Ni Foam scaffold.

3.2.2 Electrodeposition of Gold Nanoparticles

The electrodeposition of AuNPs on GF was carried out in a 2 mM $HAuCl_4$ solution using a conventional three-electrode configuration comprising of GF, Ag/AgCl and a platinum wire as working, reference and counter electrodes, respectively. In the process, Au (III) ions were reduced onto GF at a fixed DC potential of -0.2 V for a short time of 30 s to form AuNPs as depicted in Fig. 3.1d.

3.2.3 Characterizations

The surface morphology of Au-decorated GF was examined by field-emission scanning electron microscopy (FE-SEM: Hitachi, SU-8030). The material phases of the materials were evaluated by X-ray diffraction (XRD: Rigaku, TTRAXIII) using Cu Kα radiation (30 kV, 15 mA) at a detecting speed of 3°/min. The related chemical bonding was characterized by Raman spectroscopy (Renishaw: inVia Qontor Raman microscope) using a 2.5 mW laser with an excitation wavelength of 633 nm.

3.3 SAM Formation

We applied Self-Assembled-Monolayer (SAM) and 11-mercaptoundecanoic acid (11-MUA) to assist antibody decoration on the GF/AuNPs surface. GF/AuNPs electrode were immersed in 10 mM 11-MUA in ethanol-dissolved solution for 22 hours. SAM is thus formed on surface of the electrode on AuNPs deposited sites using thiol-group binding. After that the GF/AuNPs/SAM was rinsed with ethyl alcohol to remove all unbound compounds. EDC (50 mM) and NHS (50 mM) are added on purpose of antibody-attachment. This formed immobilized SAM ending with carboxylic group. Electrode material is now ready to be decorated with NGAL antibody as described in the following section.

3.4 Lipocalin-2 Antibody Addition

Anti-LCN2 and NGAL solution were purchased from Sigma-Aldrich. Anti-LCN2 coated on the surface electrode using thiol and carboxylic-ending group on gold nanosites. 5 ml volume of 10 mg/ml Anti-LCN2 were added to coat the active electrode area. Phosphate Buffer Solution (PBS, pH =7.2) of 0.2 M was prepared from Na_2HPO_4 and NaH_2PO_4. NGAL solution at different concentrations was freshly prepared within less than 20 minutes before each experiment. Bovine Serum Albumin (BSA, 0.1%) was dissolved in 0.2 M PBS (pH 7.2) to serve as blockers for non-specific binding sites. Anti-LCN2 is applied on GF/AuNPs electrodes for two hours. The LCN2 antibody is immobilized on AuNPs and graphene layer using electrostatic force. UV-Vis absorption is carried out before and after applying Anti-LCN2. Localized-Surface-Plasmon Resonance (LSPR) peaks was shifted from 545 nm for bare GF/AuNPs to 558 nm for Anti-LCN2 functionalized GF/AuNPs.

3.5 Electrochemical Measurements

All the electrochemical measurements were performed using the same three-electrode system as that of electrodeposition. The cyclic voltammetry was conducted in the presence of ferri/ferrocyanide redox in 0.1 M KCl with the potential window ranging from ~0.5 to ~0.75 V in NGAL solutions with various concentrations of 0–210 ng/ml. All solutions were prepared in phosphate buffer saline (PBS, pH = 7.2). Amperometric detections of NGAL were also performed at a fixed applied potential of 0.66 V by adding predetermined amounts of the NGAL stock solution (1 μg/ml) into the electrochemical cell. For specificity evaluation, two interfering organic chemicals including uric acid and creatinine were added after amperometric detections of NGAL at a high concentration of 100 ng/ml.

CHAPTER 4
RESULTS

This chapter reports NGAL electrochemical determination results. Diffferent NGAL concentrations was diluted in fixed buffer solutions. First, CV was conducted. Second, by picking up a reduction potential at 0.66 V, chronoamperometry was done to determine NGAL concentration. Sensitivity and precision will be reported. Its interference test was carried out by dropping uric acid and creatinine into the solution showing negligible interfering current.

Figure 4.1

Cyclic Voltammograms (a-b) EIS Nyquist Plot (c-d) Linear fit and comparison (e-f).

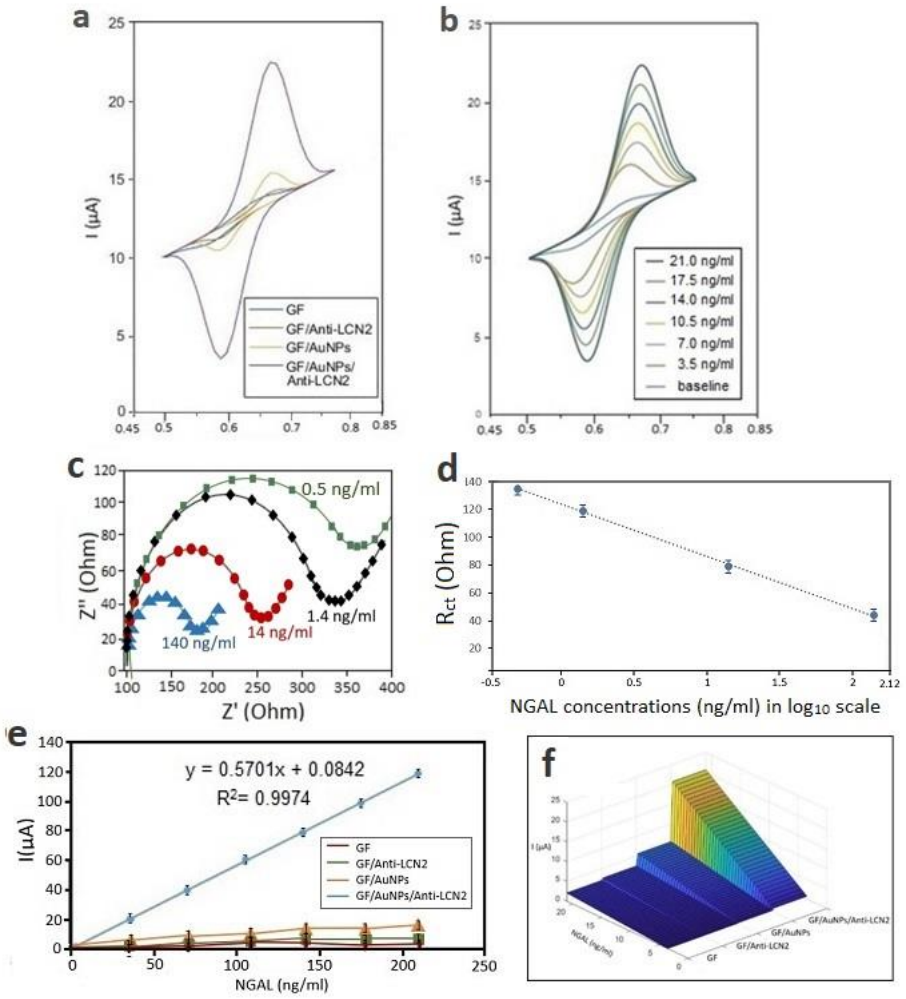

Note that, figure 4.1a reported Cyclic Voltammograms of 21 ng/ml NGAL with 2 mM $Fe(CN)_6^{3-}$/$Fe(CN)_6^{4-}$ with in 0.2 M PBS (pH=7.2) and 0.1 M KCl using different electrodes: GF, GF/Anti-LCN2, GF/AuNPs and GF/AuNPs/Anti-LCN2. Figure 4.1b were the Cyclic Voltammograms of GF/AuNPs/Anti-LCN2 in NGAL solutions with various concentrations ranging from 0 to 21 ng/ml in the presence of 2 mM $Fe(CN)_6^{3-}$ /$Fe(CN)_6^{4-}$ in 0.2 M PBS (pH=7.2) and 0.1 M KCl. Note that the baselines of different electrodes were adjusted to the same level for the purpose of comparison. Figure 4.1c was the acquired Electrochemical impedance spectroscopy (EIS) in Nyquist plot mode for 0.5 ng/ml, 1.4 ng/ml, 14 ng/ml, and 140 ng/ml NGAL respectively (in the presence of specified buffers). Figure 4.1d showed Log-linear relationship between NGAL concentration and electron transfer resistance – an extended detail of Fig 4.1c. Figure 4.1e reported an extended measurement plot, baseline-subtracted oxidation current vs. NGAL concentration of GF/AuNPs/Anti-LCN2. Meanwhile, GF/AuNPs without antibody (not appearing in the Figure) saturates at negligibly low current and cannot linearly scale up in ng/ml measurement. Figure 4.1f showed surface plot showing redox peak current amplitudes vs NGAL concentrations in different electrodes.

4.1 Electrochemical Sensing Characteristics

Fig. 4.1a compares the CV responses of GF, GF/Anti-LCN2, GF/AuNPs and GF/AuNPs/Anti-LCN2 towards a 21 ng/ml NGAL solution. Evidently, GF/AuNPs exhibit much higher reduction and oxidation peaks at 0.58 and 0.66 V compared with SCPE/AuNPs and GF, respectively. The results demonstrate that the copresence of GF and AuNPs leads to synergistically enhanced electrochemical sensitivity to NGAL. The CV responses of GF/AuNPs to various NGAL concentrations are demonstrated in Fig. 4.1b. However, 210 ng/ml was not plotted in Fig. 4.1b because it will dominate and details at low concentration would disappear. It shows that the magnitudes of CV redox peaks increase monotonically with increasing NGAL concentration. In addition, the location of oxidation peak potential slightly increases as the NGAL concentration increases, which can be corresponding to increasing diffusion resistance of NGAL. Ferri/Ferrocyanide act as the mediator between electrode and NGAL. Electrons are transferred from NGAL to GF electrode via $[Fe(CN)_6]^{3-}$/$[Fe(CN)_6]^{4-}$ and vice versa. Comparing the surface area ratio between AuNP sites and GF, the parts that electron transfer from NGAL through Anti-LCN2 and AuNPs/GF are negligible comparing with

the amount that electons transfer through Graphene/Nickel foam directly via $[Fe(CN)_6]^{3-}$/ $[Fe(CN)_6]^{4-}$ as the mediator. Thiolated NGAL Antibody acts as the attractor for NGAL so that it becomes closer to GF surface and act massive electron transfer through GF surface. This platform conceptually achieves greater sensitivity than letting NGAL move randomly near and far from the electrode surface. Fig. 4.1c shows Impedance Spectroscopic Nyquist plot for 0.5 ng/ml, 1.4 ng/ml, 14 ng/ml, and 140 ng/ml NGAL respectively (in presence of ferri/ferrocyanide, KCL and PBS as described). The more analyte concentration, the lower etectron-transfer impedance as seen in the Nyquist plot. Electron-transfer current is thus proportional to NGAL concentration. This correlation occurs because 3D graphene foam has no analyte-stacking effect because of its extraordinary large surface area in the microporous structure. The structure has magnificently more surface area compared to solid electrode like screen-printed carbon films, solid gold electrode, etc. The extended response signals taken as the CV oxidation peak currents above the baseline of all electrodes are plotted as a function of NGAL concentration as displayed in Fig. 4.1d showing linearity in log scale. The current signals of all electrodes are linearly proportional to NGAL concentrations in the range of 0.05-210 ng/ml. Additionally, the GF/AuNPs sensor offers a relatively high sensitivity of 0.574 μA per ng/ml and a low detection limit of 0.042 ng/ml. Moreover, the current signal exhibits a very small standard deviation (SD) of 0.007 μA corresponding to a current precision value of +/- 2SD = 0.014 μA and +/- 0.025 ng/ml in term of NGAL concentration, confirming high stability and good repeatability.

Figure 4.2

Amperometric detection using different electrodes: GF/AuNPs/Anti-LCN2, GF/Anti-LCN2, GF/AuNPs and GF respectively with (a) successive additions of NGAL solutions at different concentrations and (b) addition of 100 ng/ml NGAL, 1 mM uric acid (UA) and 0.1 M creatinine (Cr).

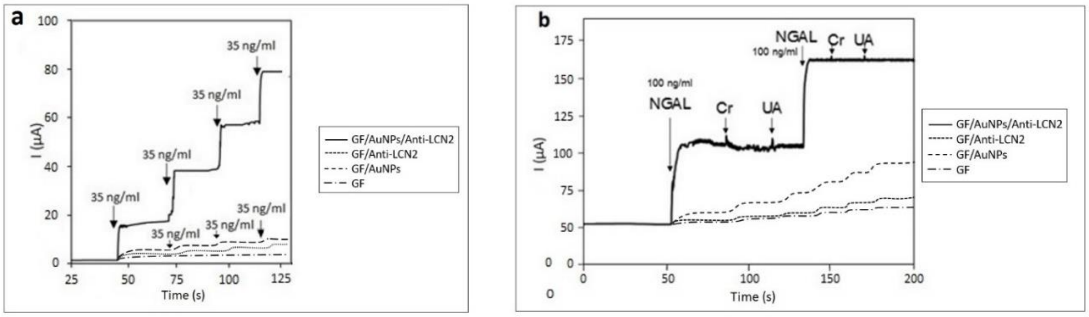

The chronoamperometric detection behaviors of GF/AuNPs/Anti-LCN2 electrode at the oxidation peak potential of 0.66 V at various NGAL concentrations and varying electrode materials were illustrated in Fig. 4.2a. GF/AuNPs/Anti-LCN2 shows highest sensitivity while GF/AuNPs works better than GF/Anti-LCN2 because Anti-LCN2 cannot bind with GF without thiol group. With the stepwise addition of 35 ng/ml, the current increases ~17-19 μA per step with short response times of less than 50 ms. The chronoamperometric current responses are in accordance with the CV responses in Fig. 4.2(a-b). The interference results tested in this detection mode are presented in Fig. 4.2b with various electrodes. Other materials except GF/AuNPs/Anti-LCN2 show non-selective behavior to NGAL, they also response to uric acid and creatinine. This result proves that GF/AuNPs/Anti-LCN2 yields high sensitivity (Fig 4.2a) and highest selectivity (Fig 4.2b) compared to other electrodes in the experiment. It is evident that the additions of 1 mM Uric Acid (UA) and 0.1 mM Creatinine (Cr) yield only small unsteady current spike after adding 100 ng/ml NGAL, which caused step currents of ~52-54 μA. Since the concentrations of UA and Cr are much higher than that of NGAL, it can be concluded that UA and Cr, potential interfering species in urine, does not interfere the amperometric NGAL detection of GF/AuNPs/Anti-LCN2 electrode, implying that the electrode is selective for NGAL detection in urine samples.

The achieved NGAL detection limit of 0.042 ng/ml is magnificantly better than that of previously described AuNPs immunosensor for NGAL detection (Kannan, Tiong & Kim, 2012). Additionally, the attained linear range of 0.05-210 ng/ml covers the normal urinary NGAL level of 5.7-17.7 ng/ml as well as the threshold values of 50-100 ng/ml for AKI in human serum and urine (Mishra *et al.*, 2005). Furthermore, the GF/AuNPs sensor exhibits high NGAL specificity, stability and repeatability. Consequently, the GF/AuNPs electrode is highly promising for label-free detection of urinary NGAL and early diagnosis of AKI.

Limit of detection (LOD) is computed by standard formula 3.3SD/*s* where sensitivity *s* = slope between response current and analyte concentration. Substituting *s* = 0.5701 μA.ml/ng and SD = 0.007256 μA we achieved LOD = 3.3*(0.007256)/0.5701 = 42 pg/ml.

4.2 Sensing Mechanisms

The GF/AuNPs platform provides ultra-high sensitivity for electrochemical NGAL detection due to three possible mechanisms. Firstly, large surface area of 3D graphene foam enhances the density of AuNPs and electrochemical effective surface area. Secondly, the electric dipoles on 3D graphene/Ni foam (Fig. 4.3a) enhance the adsorption of amine group of NGAL. The interface dipole layer between graphene and nickel in three-dimensional further may amplify the redox currents and thus greatly improve the electrochemical sensitivity (Zhang, *et al.,* 2018). In addition to Zhang, *et al.,* (2018), our work employed triple interlayer dipoles of graphene-nickel-gold to further enhance electron transfer. Analyte-stacking does not affect linear range of sensing since gigantic surface of GF of reaction support large analyte concentrations. LCN2 Antibodies attract the analyte (NGAL) into AuNPs sites lying on top of GF surface. Then massive electron transfer occurs between NGAL and Graphene/Nickel foam due to interlayer dipole enhancement. NGAL could be distributed into multiple sites of 3D graphene foam and this describes broad linearity range of the sensing.

Figure 4.3

Sensing Mechanisms: (a) An Interface Dipole Layer between Graphene and Nickel of GF and (b) Bindings of NGAL and Anti-LCN2 with Electron Transfer Simultaneously among Gigantic Sites per Mass of GF/AuNP/Anti-LCN2.

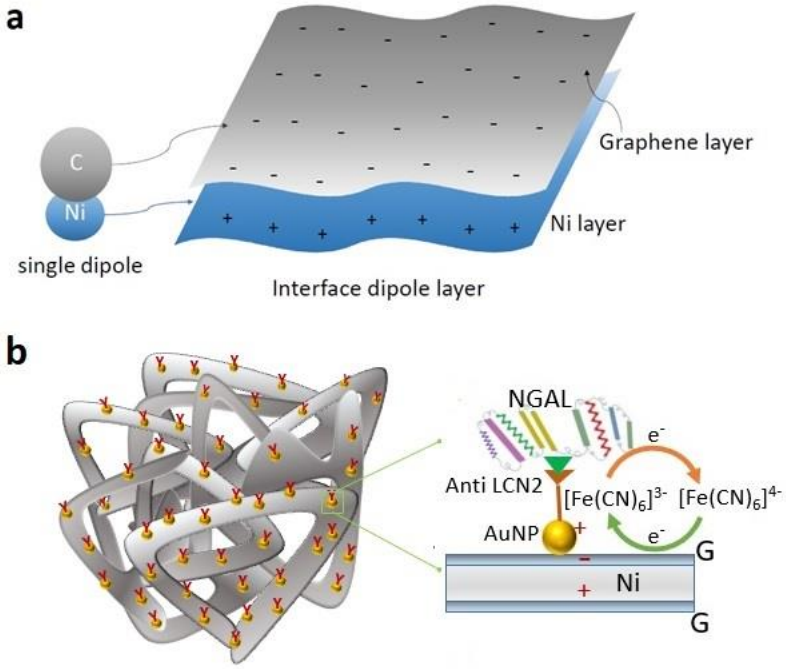

Table 4.1

Reproducibility of the Platform, Showing its Standard Deviations of Repeated Experiments, SD Showing Average SD of 3 NGAL Concentrations (1.4 ng/ml, 105 ng/ml, and 210 ng/ml) Experiments, with 5 Repetitions Each.

Experiments	Value	SD
CV	I (µA)	0.007 µA
EIS	R_{ct}	6.42 Ohm
Amperometry	I (µA)	0.012 µA

Repeatability is summarized in table 4.1, showing SD of 5 repetitions for each NGAL concentrations, where SD is averaged among SD of each different NGAL concentration experiments.

Table 4.2

Comparison of LOD and Linearity Range Between Different Electrode Materials in Literatures and This Work.

Materials	LOD	Linearity Range	Reference
Gold electrode/AuNPs/PAMMAM immunosensor	1 ng/ml	50-250 ng/ml	Kannan, Tiong & Kim, (2012)
CBN/immunosensor	0.37 pg/ml	0.001-10 ng/ml	Chen & Lu (2018)
Carbon + enzyme-based sandwiches	97 pg/ml	0.15-2 ng/ml	Neves et. al. (2020)
Affinity peptide-incorporated	1.74 ng/ml	1-100 μg/mL	Cho *et. al.* (2019)
graphene/polyaniline SPCE	21.1 ng/ml	50-500 ng/ml	Yukird *et al.* (2019)
GSPE/P(ATT)-GO/AuNPs	0.3 ng/ml	1.0-1000.0 ng/ml	Tığ & Ş. Pekyardımcı (2019)
GF/AuNPs/SAM/immunosensor	42 pg/ml	0.05-210 ng/ml	This work

In table 4.2, we compare the performances of our proposed platform and the other materials in literature. Our platform keep balancing between low detection limit and wide linearity range, which are not the cases in other platforms. Ultra-high sensitivity was achieved due the electromagnetic dipole enhancement between Nickel and graphene layers while thiolated antibodies attract the NGAL to the active surface sites so that a large number of electron transfer can occur between NGAL and GF.

CHAPTER 5

REPEATABILITY AND MEASUREMENT ON HUMAN URINE NGAL

This chapter reports reproducibility test and validation of our platform on actual urine samples' NGAL was determined. Relationship between actual human urine NGAL and amperometric current was form as one-directional function (described in this chapter). Our platform was tested for its repeatability as shown in figure 5.1. Precision was +- 0.5 ng/ml (at +/- 0.96SD, 95% confidence).

5.1 Repeatability and Performance vs Standard ELISA

ELISA detection kit for NGAL was purchased from Sigma Aldrich, and the dilution and back-conversion for NGAL determination was done as standard guideline. A real urine sample with known NGAL values was brought from a CKD patient with a signed consent and pre-measured NGAL concentrations. Sample were kept at -32 ℃ before it was defrosted for the experiment. Samples beginning with 240 ng/ml stock is diluted into multiple concentrations as shown in the graphs in Fig. 5.1a. showing linear fit of standard ELISA kit for NGAL and our GF/AuNPs/Anti-LCN2 platform.

Figure 5.1

This Work Compared to Standard ELISA Sensing for NGAL in Actual Urine Samples (a) Comparing Linear Regression between two Methods (b) Bland-Altman Plot of our Platform Compared with Standard ELISA Showing Majority of Errors Are Between +/- 1.96SD.

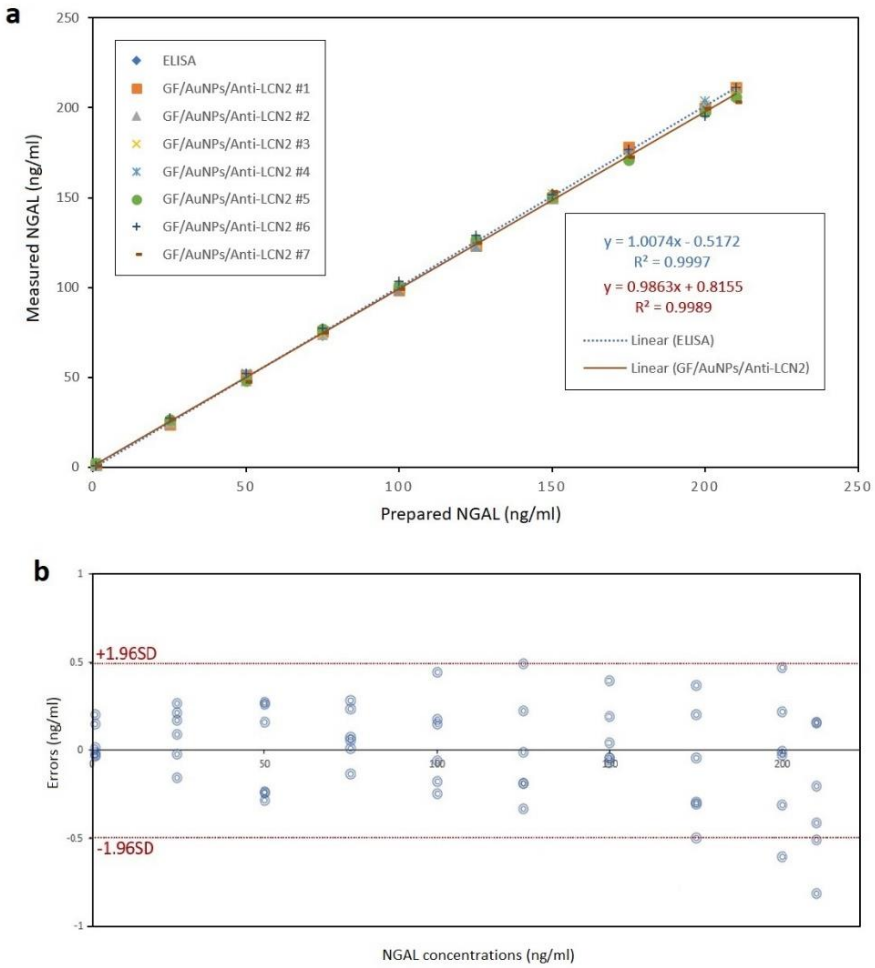

The results show acceptable correlation between our platform and standard ELISA. Validation of our platform can be illustrated in the Bland-Altman plot (Fig. 5.1b) showing that at 95% confidence the errors are between +/- 1.96 SD where SD = 0.25 ng/ml. Errors were computed between standard ELISA and the NGAL determination from GF/AuNPs/Anti-LCN2 electrode. It was observed that the absolute errors would increase as the concentration increases but the percentage of errors would still be the same, as previous work has reported (Oldham, Myland & Bond, 2012).

5.2 Validation of our AuNP/GF/Anti-LCN2 Platform at Trace NGAL Level

Validation was performed with actual urine samples. The amperometric detection shown that measured current is linearly proportional to NGAL concentration in ng/ml scale where detection limit can go down to ~50 pg/ml. Measurement was carried out by dropping 50 uL urine into 5ml solution of 0.2 M PBS (pH 7.2) and ferri/ferrocyanide. Amperometric detection was shown in figure 5.2.

Figure 5.2

Amperometric Detection After Dropping Actual Urine Samples 50µl Each onto 5 ml Buffer Solutions lying on a Magnetic Stirrer and Using GF/AuNPs/Anti-LCN2 as the Working Electrode

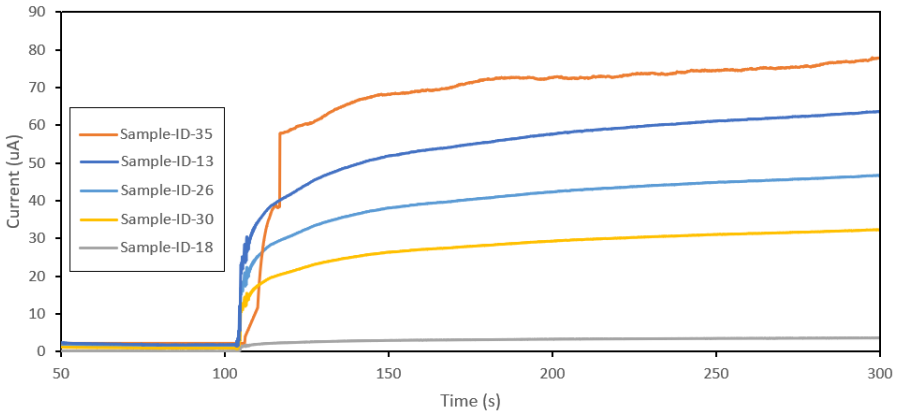

Figure 5.3

Five Urine Samples at Trace level Below 6 ng/ml.

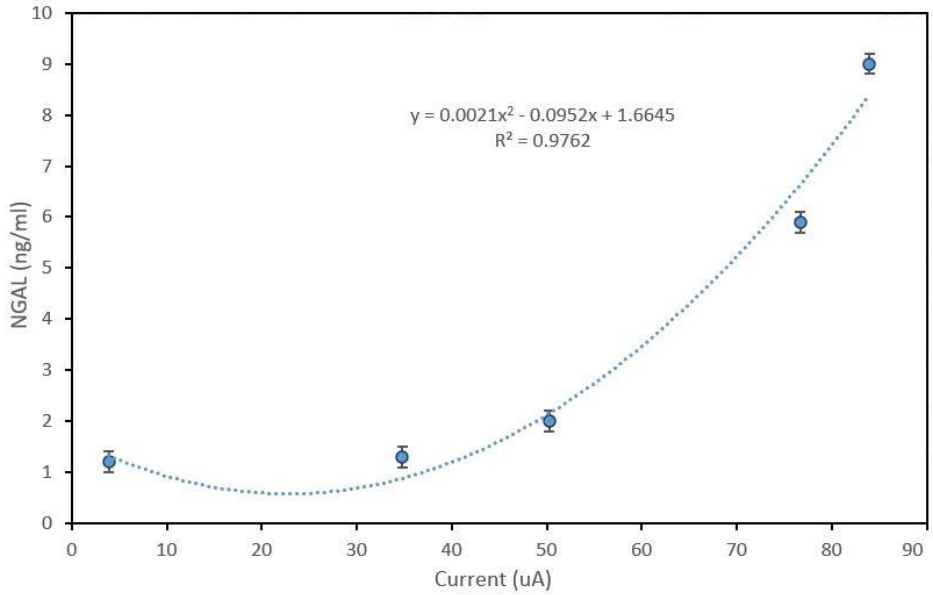

To sum up, NGAL measurement in actual urine samples using our platform. It shown that one directional function can be formed with satisfied accuracy according to Bland-Altman plot (see Fig. 5.1b). Second-order polynomial function can be used to fit the Sensing in actual human urine NGAL. In these trace amount of NGAL (1-9 ng/ml), the curve is non-linear in this range. Actually, NGAL and current relationship does not require linearity. Only if there is a function f(I) mapping from measured current to the NGAL concentration, the sensing model can be formed for each readout current value. For broader range, further investigations required to model the accurate functional relation between the readout current and the NGAL concentration in actual human urine.

CHAPTER 6
CONCLUSION AND FUTURE OUTLOOK

6.1 Conclusion

In conclusion, the GF/AuNPs fabricated by CVD and electrodeposition processes were investigated for electrochemical detection of NGAL. The GF/AuNPs/Anti-LCN2 electrode offered an ultra-low NGAL detection limit of 42 pg/ml, linear range of 0.05-210 ng/ml, high stability, good repeatability and very selective. Broad linear range supports rapid detection since sample does not require dilution and back-conversion steps like the limited linear range cases. The attained performances might be attributed to large specific surface area of GF and AuNPs which prevent analyte stacking effect that normally cause limited linear range in screen-printed and rod-shaped sensors. NGAL antibody functionalized on GF/AuNPs serve to achieve great selectivity. Specificity was tested and satisfied against uric acid and creatinine interference as seen in chronoamperometry. Gigantic surface area of 3D foam increases active area for electrostatic binding of Lipocalin-2 antibody and thus linearity range can be scale-up by adding more antibodies. There is no stacking effect of NGAL when the NGAL concentration increase since 3D GF has significantly more active surface area compared to other flat-shaped or rod-shaped electrodes. Furthermore, AuNP-Graphene-Ni layers form multiple dipole layer which greatly enhance electron mobility and to achieve ultra-sensitivity compared to other plain electrodes. Meanwhile, Anti-LCN2 acts to attract NGAL into AuNPs sites lying on top of GF surface where large charge transfer can occur between NGAL and GF. In chapter 5, our platform was test in actual human urine samples and detection limit achieved was ~50 pg/ml for those samples where functional detection was formed for 1-9.5 ng/ml range. Therefore, the GF/AuNPs/Anti-LCN2 platform was promising as an ultra-sensitive and highly specific NGAL electrochemical sensor for non-invasive AKI diagnosis.

6.2 Future Outlook

Design for actual applications as urine NGAL sensor strip is shown in figure 6.1. Our material GF/AuNPs/Anti-LCN2 is placed as the working electrode in ordinary electrochemical strip (Fig. 6.1a) and its numerical reader (Fig. 6.1b). Autopipette can be used to draw urine and dropped at the working electrode inside the sensing strip.

Figure 6.1

Designed Electrochemical Sensor Strip for Urine NGAL Determination. (a) Dropping of Urine Sample onto GF/AuNP/Anti-LCN2 Electrode (b) Digital Readout and Display

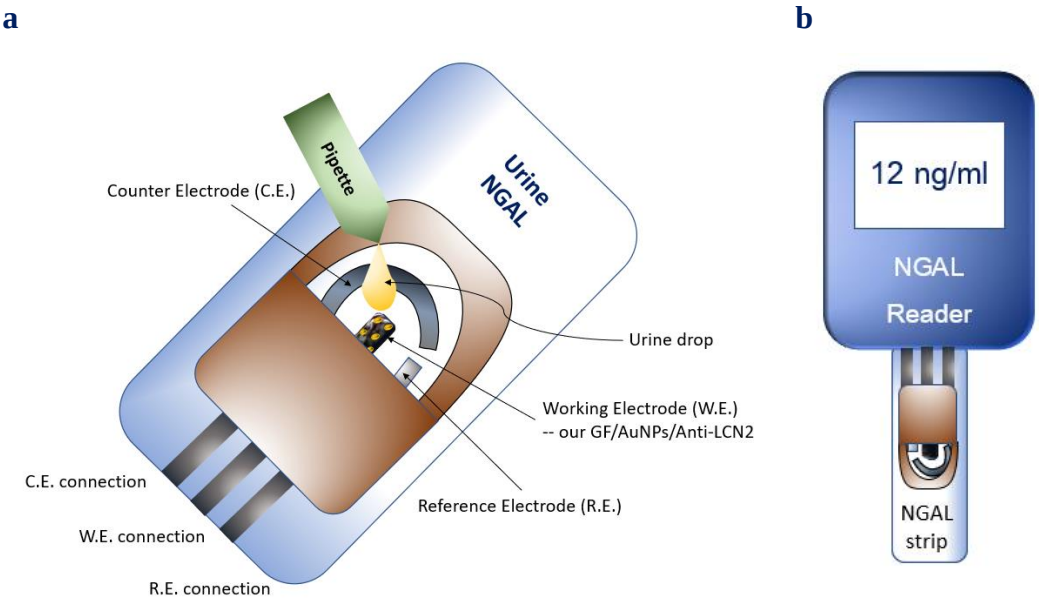

Our research platform is put as the working electrode on which urine will be dropped (see Figure 6.1). C.E., W.E. and R.E. connections will be connected to a handheld reading devices showing numeric NGAL concentration on an OLED or LCD display. For future improvement of accuracy in clinical applications, which is not in the current scope, machine learning can be incorporated and personal medical features such as blood pressure, BMI, existed disease, etc. can be included as well as current readout to form a precise model of clinical NGAL determination.

REFERENCES

Cruz, D. N. *et al.* (2010). Plasma neutrophil gelatinase-associated lipocalin is an early biomarker for acute kidney injury in an adult ICU population. *Intensive Care Med,* 36**,** 444-451. https://doi.org/10.1007/s00134-009-1711-1

Nickolas, T. L. *et al.* (2012). Diagnostic and prognostic stratification in the emergency department using urinary biomarkers of nephron damage: a multicenter prospective cohort study. *J. Am. Coll. Cardiol,* 59, 246-255. https://doi.org/10.1016/j.jacc.2011.10.854

Makris, K. and Spanou, L. (2015). Acute Kidney Injury: Definition, Pathophysiology and Clinical Phenotypes. *Clin. Biochem.* 48(18), 1291-1297. https://www.ncbi.nlm.nih.gov/pmc/articles/PMC5198510/

Mishra, J. *et al.* (2005). Neutrophil gelatinase-associated lipocalin (NGAL) as a biomarker for acute renal injury after cardiac surgery. *Lancet* **365** 1231-1238. https://doi.org/10.1016/s0140-6736(05)74811-x

Novoselov, K. S. *et al.* (2004). Electric field effect in atomically thin carbon films. *Science,* 306, 666-669. https://doi.org/10.1126/science.1102896

Ma, Y. *et al.* (2014). 3D graphene foams decorated by CuO nanoflowers for ultrasensitive ascorbic acid detection. *Biosens. Bioelectron.*, 59, 384-388. https://doi.org/10.1016/j.bios.2014.03.064

Wu, S., He, Q., Tan, C., Wang, Y. & Zhang, H. (2013). Graphene-based electrochemical sensors. *Small,* 9**,** 1160-1172. https://doi.org/10.1002/smll.201202896

Chen *et al.*, Z. (2011). Three-dimensional flexible and conductive interconnected graphene networks grown by chemical vapour deposition. *Nat. Mater.* **10**, 424. https://doi.org/10.1038/nmat3001

Zhang, L. L., Zhou, R. & Zhao, X. S. (2010). Graphene-based materials as supercapacitor electrodes. *J. Mater Chem,* **20,** 5983-5992. https://doi.org/10.1039/C000417K

Stoller, M. D., Park, S., Zhu, Y., An, J. & Ruoff, R. S. (2008). Graphene-based ultracapacitors. *Nano Lett.,* 8**,** 3498-3502. https://doi.org/10.1021/nl802558y

Zhang, C. *et al.* (2018). Catalytic mechanism of graphene-nickel interface dipole layer for binder free electrochemical sensor applications. *Comm. Chem.*, 1, 94. https://doi.org/10.1038/s42004-018-0088-x

Yue, H. Y. *et al*. (2020). Highly sensitive and selective dopamine biosensor using Au nanoparticles-ZnO nanocone arrays/graphene foam electrode. *Mater. Sci. Eng. C*, 108, 110490. https://doi.org/10.1016/j.msec.2019.110490

Guo, X. *et al.* (2020a). A sensitive method to determine dopamine in the presence of uric acid based on In2O3 nanosheet arrays grown on 3D graphene. *Microchim. Acta*, 187, 218. https://doi.org/10.1007/s00604-020-4199-6

Guo, X. *et al.* (2020b). In_2S_3 nanosheet arrays grown on the 3D graphene for sensitive detection of epinephrine in the presence of uric acid. *J Mater Sci: Mater Electron,* 31, 3549–3556. https://doi.org/10.1007/s10854-020-02903-z

Perumal, V. *et al.* (2018). Gold nanorod embedded novel 3D graphene nanocomposite for selective bio-capture in rapid detection of Mycobacterium tuberculosis. *Biosens Bioelectron*. 116, 116-122. https://doi.org/10.1016/j.bios.2018.05.042

Ong, C. C. *et al.* (2020). Iron nanoflorets on 3D-graphene-nickel: A 'Dandelion' nanostructure for selective deoxynivalenol detection. *Biosens. Bioelectron.*, **154**, 112088. https://doi.org/10.1016/j.bios.2020.112088

Kannan, P., Tiong, H. Y. & Kim, D. H. (2012). Highly sensitive electrochemical determination of neutrophil gelatinase-associated lipocalin for acute kidney injury. *Biosens. Bioelectron.,* 31, 32-36. https://doi.org/10.1016/j.bios.2011.09.036

Chen, Z. & Lu, M. (2018). Thionine-coordinated BCN nanosheets for electrochemical enzyme immunoassay of lipocalin-2 on biofunctionalized carbon-fiber microelectrode. *Sens. Actuators B Chem.,* 273**,** 253-259. https://doi.org/10.1016/j.snb.2018.06.053

Neves, M. M. P. S., Nouws, H. P. A., Santos-Silva, A. & Delerue-Matos, C. (2020). Neutrophil gelatinase-associated lipocalin detection using a sensitive electrochemical immunosensing approach. *Sens. Actuators B Chem.,* 304**,** 127285. https://doi.org/10.1016/j.snb.2019.127285

Srichan, C. *et al.* (2016). Highly-Sensitive Surface-Enhanced Raman Spectroscopy (SERS)-based Chemical Sensor using 3D Graphene Foam Decorated with Silver Nanoparticles as SERS substrate. *Sci. Rep.,* 6, 23733. https://doi.org/10.1038/srep23733

Cho, C. H., Kim, J. H., Song, D.K., Park, T. J. & Park, J. P. (2019). An affinity peptide-incorporated electrochemical biosensor for the detection of neutrophil gelatinase-associated lipocalin. *Biosens. Bioelectron*., 142**,** 111482. https://doi.org/10.1016/j.bios.2019.111482

Yukird, J. *et al.* (2019). Label-free immunosensor based on graphene/polyaniline nanocomposite for neutrophil gelatinase-associated lipocalin detection, *Biosens. Bioelectron.*, 87, 249-255. https://doi.org/10.1016/j.bios.2016.08.062

Tığ, G. A. & Pekyardımcı, Ş. (2019). An electrochemical sandwich-type aptasensor for determination of lipocalin-2 based on graphene oxide/polymer composite and gold nanoparticles. *Talanta,* 210, 120666. https://doi.org/10.1016/j.talanta.2019.120666

Sur, U. K. (2012). "Graphene: A Rising Star on the Horizon of Materials Science", International Journal of Electrochemistry, 2012, 237689, 1-12. https://doi.org/10.1155/2012/237689

Oldham, K. B., Myland, J. C. and Bond, A. M. (2012) “Electrochemical Science and Technology: Fundamentals and Applications”, John Wiley & Sons.